Published in final edited form as:
Microbes Infect. 2004 October ; 6(12): 1063–1072. doi:10.1016/j.micinf.2004.06.002.

The human and mouse orthologous LIM-only proteins respectively encoded in chromosome 6 and 17 show a different expression pattern

Armanda Casrouge[a], **Reiner Veitia**[b], **Jacqueline Kirchner**[c], **Michael. J. Bevan**[c], and **Jean Kanellopoulos**[d,*]

[a] Laboratoire de Biologie Moléculaire du Gène, Inserm U277-Institut Pasteur, 75724-Paris cedex 15, France

[b] Immunogénétique humaine, Institut Pasteur, Université Denis Diderot, Paris, France

[c] Department of Immunology, Howard Hughes Medical Institute, University of Washington, Seattle, WA 98195, USA

[d] Laboratoire Activation Cellulaire et Transduction des Signaux, IBBMC, CNRS-UMR 8619, Université Paris-Sud Centre d'Orsay, 91405 Orsay cedex, France

Abstract

Thymocytes interact with various subpopulations of thymic epithelial cells (TECs) at different stages of their development. To identify new molecules specifically expressed in TECs and/or thymic nurse cells (TNCs), we used representational difference analysis. We identified a LIM protein located on mouse chromosome 17 (m17TLP) and belonging to the family of the LIM-only proteins (LIMo). We found a new splice variant in addition to the two describedA and B isoforms. The three alternative species of m17TLP are found strictly in the thymic stroma. This protein is expressed on a subpopulation of TECs and TNCs. Strikingly, we found that the human ortholog of m17TLP, located on chromosome 6 (h6LIMo), is expressed in most tissues, but not in skeletal muscle. We have identified four human splice variants of h6LIMo which differ in their carboxy-terminal regions. The sequence comprising the genomic structure suggests that CRP2 is the closest known relative of m17TLP. Although the human and mouse nucleotide sequences are 88–97% homologous, this homology is reduced to 47% in the promoter regions, which strongly suggests that their differential expression is related to their promoter regulatory activity.

Keywords

LIM-only protein; LIM domains; Thymus; Representational difference analysis; Thymic epithelial cells; Thymic nurse cells

1. Introduction

Proteins containing LIM domains seem to be involved in many biological processes, such as cytoskeleton organization, organ development and oncogenesis. The LIM motif is a cystein–histidine-rich, zinc coordinated domain, comprising two zinc fingers with the consensus sequence CX2CX16-23HX2CX2CX2CX16-23CX2-3(C/H/D) [1,2]. Unlike DNA-binding zinc finger proteins, the LIM domains do not bind DNA but mediate specific protein–protein

*Corresponding author. Tel.: +33-1-69-15-48-25; fax: +33-1-69-85-37-15. jean.kanellopoulos@ibbmc.u-psud.fr (J. Kanellopoulos).

interactions. Various proteins with LIM domains have been identified. They belong to four families, among which the LIM-only proteins (LIMo) do not possess a kinase domain or a homeodomain [3,4]. Among the LMo proteins, four cystein-rich proteins (CRP) encoded by different genes have been identified in vertebrates: CRP1, CRP2, CRP3/MLP and thymus LIM protein (TLP) [5]. The CRPs interact with α-actinin and zyxin [6,7]. The latter contains three LIM domains, a nuclear export signal and a proline-rich region [8].

The thymic stroma is required for T cell development and provides a complex microenvironment in which many sub-populations of cells interact with thymocytes (reviewed in [9]). Bone-marrow-derived cells colonize the thymus and give rise to thymocytes and dendritic cells. Immature thymocytes are found mainly in the thymic cortex, where they proliferate. Positive selection of thymocytes is triggered by the interaction of their surface receptor for antigen (TCR) and peptide/MHC complexes expressed on cortical epithelial cells. Negative selection is mainly mediated by dendritic cells found in the medulla and at the corticomedullary junction of the thymus, and to a lesser extent, by medullary epithelial cells. This process of selection eliminates from the pool of thymocytes those, which have too high an avidity for self-peptide/MHC complexes, thus purging the immune system from potentially harmful T cells.

Schematically, three types of thymic epithelial cells (TECs) have been characterized by their morphology and with various monoclonal antibodies: subcapsule/trabeculae, cortex and medulla (reviewed in [9]). The first group of TEC is MHC class II negative and labeled with clusters of thymic epithelial staining (CTES II) monoclonal antibodies. Cortex TECs are subdivided in three groups of epithelial cells, which are stained with pan-cortex CTES III monoclonal antibodies and bear major histocompatibility complex (MHC) class II molecules.

Thymic nurse cells (TNCs) were identified by Wekerle et al. in 1980 [10]. They are located in the cortical region of the thymus. TNCs are multicellular complexes comprising one epithelial cell that envelops thymocytes in vacuoles surrounded by the epithelial cell membrane. TNCs have been found in human, murine, avian and amphibian species. These cells express on their surface MHC class I and II molecules but no specific markers of thymocytes such as CD4, CD8. TNCs are not phagocytic cells, since the thymocytes, which they contain, appear viable. It has been postulated that TNCs provide a microenvironment for selection of thymocytes. In the chicken, functional studies showed that thymocytes included in TNCs were reacting against both allogeneic and syngeneic targets [11]. These results suggested that thymocytes inside TNCs have been positively selected on self-MHC molecules but did not undergo negative selection. It was also shown that mouse TNCs present self-peptides, i.e. they stimulate a T cell hybridoma specific for hemoglobin [12]. It has been claimed that TNCs were in vitro artifacts; however, TNC-like structures have been observed in human [13] and in murine thymus [14, 15]. Up to now, the exact function of TNCs has remained elusive; some reports favor a role of TNCs in thymocyte maturation, whereas others establish TNCs as a site of thymocyte apoptosis [16,17]. Recently, it was shown that a trans-sialidase from *Trypanosoma cruzi*, the causative agent of Chagas' disease, induces a profound but transient decrease in $CD4^+CD8^+$, $CD4^+$ and $CD8^+$ thy-mocyte subpopulations [18]. Furthermore, the *T. cruzi* trypomastigote-derived trans-sialidase was shown to induce apoptosis in the TNC complex [18]. Thus, we used the method of "representational difference analysis" (RDA) [19,20] to identify genes specifically expressed in TNCs or TECs.

Recently, a new LIMo protein TLP was identified in the mouse thymus [5]. TLP was found to be expressed in a subset of TECs. In mice bearing a targeted disruption of the gene encoding this new LIMo protein, thymocyte development was normal and no difference was found between $TLP^{-/-}$ and $TLP^{+/+}$ animals in the percentages of $CD4^+$, $CD8^+$, $CD4^+CD8^+$ and $CD4^-CD8^-$ subpopulations. Interestingly, there is a 30% decrease in thymocyte numbers in

$TLP^{-/-}$ mice compared to the $TLP^{+/-}$ littermates. However, no modification in positive and negative selection of thymocytes was found [5].

In this work, by a different approach, we have identified this mouse LIMo (m17TLP), located on chromosome 17 and its splice variants, which are expressed in a subpopulation of TECs and TNC only. In humans, the corresponding gene is located on chromosome 6 and shares extensive identity with the mouse gene. Interestingly, we found that the human LIMo protein (h6LIMo) and its various splice variants are not selectively expressed in the thymus, but are expressed in most tissues except skeletal muscle. In line with this, the comparison between human and mouse promoters only shows 47% identity. The structure of m17TLP and h6LIMo is compared, and their differences discussed.

2. Material and methods

2.1. Isolation of murine thymic epithelial cells

Three- to four-week-old C57BL/6 female mice were obtained from Iffa-Credo (France). Ten thymi were cut into pieces and digested by collagenase 0.2 mg/ml (Life Technologies), dispase 0.2 mg/ml (Life Technologies) and DNase 10 U/ml (Amersham) in phosphate-buffered saline solution (PBS) for 20 min at 37 °C. Four successive digestions were performed using fresh enzymes as described [21]. After four washes, cells were incubated with a mixture of biotinylated monoclonal anti-CD25, anti-CD4 and anti-CD8 from Caltag and Pharmingen, respectively, for 1 h at 4 °C. Labeled cells were removed with streptavidin dynabeads M-280 (Dynal, Oslo, Norway). The remaining fraction contained stromal cells, TNCs and triple-negative thymocytes.

2.2. Representational difference analysis (RDA)

mRNA was prepared using a Quick Prep mRNA purification kit (Amersham-Pharmacia Biotech). Double-stranded cDNA was obtained with Superscript Choice system for cDNA synthesis (Life Technologies).

cDNA was digested with the restriction enzyme *Dpn*II (New England Biolabs). Then, R12 and R24 adaptators were ligated with T4 DNA ligase (New England Biolabs) as described [22]. A 30-cycle PCR was performed with R24 primers to generate amplicons (see below). These were digested with *Dpn*II, and J12 and J24 adaptaters were ligated to “tester DNA” only [22]. “Driver DNA ” was prepared from 5 μg of mRNA of triple-negative thymocytes and intestinal epithelial cells. Then, amplicons of driver were prepared as above for tester, except that J12 and J24 adaptaters were not ligated to driver amplicon. Three adsorptions were performed with driver; PCR and enzyme treatments were done as described [22].

2.3. Primers used in RDA experiments

R12: 5′-GATCTGCGGTGA-3′.

R24: 5′-AGCACTCTCCAGCCTCTCACCGCA-3′.

J12: 5′-GATCTGTTCATG-3′.

J24: 5′-ACCGACGTCGACTATCCATGAACA-3′.

N12: 5′-GATCTTCCCTCG-3′.

N24: 5′-AGGCAACTGTGCTATCCGAGGGAA-3′.

2.4. Cloning and sequencing

Cloning of substraction products, digested by *Dpn*II, was performed into the *Bam*H1 site of pUC 18 plasmid. For sequencing purposes, PCR was carried out directly on $LacZ^{-}$ colonies with *Taq* polymerase, an RP primer and the M13–40 primer. Sequencing reactions were carried out on these products using RP primer and with the ABI PRISM Big Dye Terminator Cycle Sequencing ready Reaction Kit (Perkin–Elmer ABI, Foster City, CA). Full-length cDNAs were obtained using Gene Racer kit (Invitrogen,) as recommended by the manufacturer using primer 11-5A2-reverse (5′-CAGTCAGGGTCTTCCTGCAACGTT-3′) for the 5′ step.

2.5. Northern blot analyses

Total RNA was isolated with Trizol (Life Technologies). After electrophoresis, RNA was transferred to Hybond-N membrane (Amersham-Pharmacia Biotech) as suggested by the manufacturer. A 208-bp PCR product corresponding to the fragment 420–628 bp (following numbering of AF367970) of the shorter isoform of m17TLP was labeled by random priming using the Megaprime kit (Amersham-Pharmacia Biotech). The beta-actin probe was labeled as above.

Hybridation was performed at 42 °C overnight in 50% formamide, 6× SSC, 5× Denhardt 0.5% SDS and DNA from herring sperm 100 μg/ml. Two washes were made at room temperature in 2× SSC containing 0.1% SDS, followed by two washes in 0.1× SSC with 0.1% SDS at 50 °C for 30 min. Autoradiography was performed overnight with amplifier Transcreen HE screen (Integra/biosciences).

2.6. PCR analysis of the transcripts

Total RNA from different mouse tissues was isolated using Trizol (Life Technologies). cDNA was prepared using M-MLV reverse transcriptase (Gibco-BRL) as described by the manufacturer. Human cDNAs (MTC panel I and II) were obtained from Clontech laboratories (Palo Alto, CA).

For PCR amplification in mouse tissues (Fig. 1) and m17TLP probe:

11-5A Forward: 5′-GCTGAGAAAGTGATGTCTTTGG-3′.

11-5A Reverse: 5′-GATCTTATGTCCACTGGGTCAG-3′.

HPRT (hypoxanthine phosphoribosyltransferase) primers were used for cDNA control.

HPRT forward primer: 5′-TCAACTTTAACTGGAAAGAATGTC-3′.

HPRT reverse primer: 5′-CCAGCAAGCTGCAACCTTAACCAT-3′.

For h6LIMo probe and PCR amplification in human cDNA tissues (Fig. 4).

h6LIMo1 Forward: 5′-CTGAGGTGCCAGCGTTGCCACAA-3′.

h6LIMo1 Reverse: 5′-GATGGGAGGCCTGAGTTAGGGTG-3′.

G3DPH (glyceraldehyde-3-phosphate deshydrogenase) primers were supplied by the manufacturer.

2.7. Dot blot

Human multiple tissue expression (MTE™) Array 2 (Clontech laboratories) and Mouse RNA Master Blot™ were hybridized in Express Hyb™ solution (Clontech laboratories) with h6LIMo or m17TLP probes as described above.

2.8. Immunohistochemistry and confocal microscopy

Thymi were frozen in O.C.T. compound (Tissue-Tek Miles Inc., Elkahart, IN) in a dry ice ethanol bath, and 5-mm-thick cryosections were cut, air-dried for 2 h at room temperature and fixed in acetone for 10 min at 4 °C. The slides were washed in PBS and saturated with PBS containing 2% bovine serum albumin (BSA).

The rabbit anti-TLP serum was generated in New Zealand white rabbits by Kirchner and colleagues (2001). The antiserum was affinity-purified using an Affi-gel 10 A (Bio-Rad laboratories Hercules, CA 94547), to which a glutathione S-transferase-fusion TLP protein was coupled. The affinity-purified antibodies were dissolved in PBS–2% BSA and added to the slides for 1 h at room temperature. Fluoresceinated or rhodaminated goat anti-rabbit IgG (Immunotech, Westbrook, ME) was used to reveal cells labeled with the affinity-purified anti-TLP antibodies. The stained tissues were mounted in fluorescent mounting medium (Dako corporation, Carpintaria, CA). TECs were fixed in 4% paraformaldehyde for 30 min at 4 °C, then permeabilized in PBS–0.1% Triton X-100 for 5 min at room temperature and stained in PBS–2% BSA. In all experiments, two controls were included, one with the rabbit pre-immune serum and one with the fluoresceinated or rhodaminated goat anti-rabbit IgG.

3. Results

3.1. Representational difference analysis

In order to identify mRNA specifically expressed in TECs or TNCs, we prepared cDNA from partially purified TECs, as described in Section 2. Tester DNA was prepared from partially purified TECs, and driver was obtained from a mixture of double-stranded cDNA from intestinal epithelial cells and from enriched $CD4^{-}CD8^{-}$ negative thymocytes. After three substraction steps, differential products were analyzed on an agarose gel and showed several well-individualized bands. These PCR products were cloned into the *Bam*H1 site of the pUC18 plasmid. Six different sequences were identified corresponding to m17TLP, di-ubiquitin, synaptotagmin 1, carbonyl-reductase 2, and two unknown sequences. Nineteen sequences out of 32 corresponded to different portions of TLP. A full-length cDNA of the CRP was obtained by (5′RACE).

3.2. Different isoforms of the m17TLP

The RDA products were sequenced revealing that three different isoforms of the m17TLP were present. As shown in Fig. 1, three isoforms revealed by PCR bands of 223 (TLP-A), 283 (TLP-B) and 368 bp (TLP-C) were observed in stromal thymus only. The presence of m17TLP in stromal thymus only was confirmed by Northern blot analysis (Fig. 2).

3.3. h6LIMo ortholog is not restricted to human thymus

The m17TLP nucleotide sequence matched a human sequence found on chromosome 6. The sequence identity of the mouse and human LIMo exons is striking and ranges from 88% to 97% at the nucleotide level. We then tested different human tissues to determine whether the h6LIMo is expressed in thymus only.

As shown in Fig. 3 (panel A), the h6LIMo is expressed strongly in testis, heart, cerebellum, kidney, fetal thymus and more weakly in most tissues. In mouse, the expression of m17TLP

is limited to the thymus, and the signal is very weak on the blot (Fig. 3 panel B). This may be due to the fact that thymocytes which do not express m17TLP are in large excess compared to TECs.

3.4. Isoforms of h6LIMo

We determined the number and sequences of the human isoforms by PCR carried out on various tissue cDNA. As shown in Fig. 4, five different bands were observed after PCR. Upon sequencing, we were able to define four different isoforms, labeled A (208 bp), B (280 bp), C (404 bp), and D (151 bp) in Fig. 4. The upper band found at 498 bp contained two introns and two exons and is likely due to a DNA contamination of the tissue cDNAs. The contamination by genomic DNA of some of the cDNAs was ascertained using a couple of primers, which amplify the promoter of the FOXL2 gene (data not shown).

None of the human isoforms was found to be expressed in skeletal muscle. The isoform h6LIMo-A is strongly expressed in all tissues tested (Fig. 4), whereas isoforms D and C are weakly present in most tissues except kidney, brain (D only) and lung (C only). Isoform B is found in pancreas, heart, leukocytes and colon.

The h6LIMo-A, B, and C isoforms are very similar to the three mouse ones (Fig. 5). However, the h6LIMo-D is much shorter than the others.

The mRNAs corresponding to h6LIMo are expressed in most tissues, with the exception of skeletal muscle. Various splice variants were found, and the corresponding cDNA were cloned and sequenced. The comparison of the human and mouse genes is shown in Fig. 5. The human isoforms A, B and C use exons 1, 2, 3, 4, 5 and 6. Then, alternative splicing generates the A form, which uses exon 7 and a portion of exon 8. The B isoform uses exon 7 and exon 8 contributes one amino acid only (Fig. 6). The splice variant C comprises the complete exon 7 only. Isoform D is encoded by all six first exons, and the last amino acid is generated by exon 8 (Fig. 6). This isoform lacks the last zinc finger and seems to be expressed in every tissue except brain, kidney and skeletal muscle. Fig. 6 presents an alignment of the human and mouse amino acid sequences of the various isoforms. The amino acid residues, which differ in the human and mouse sequences are shown in red. Human and mouse isoforms A share 88.5% identity. Most of the differences are found in the region linking the two LIM domains. For isoforms B and C, differences are concentrated at the carboxy termini. The carboxy-terminal domain of human isoforms B and C differs from that of the mouse because the human exon 7 contains a nucleotide sequence of 37 bp absent in the mouse gene. This 37-bp sequence generates a decapeptide in isoforms B and C, which does not correspond to any known protein motif. The mouse isoform C is composed of 256 amino acid residues and contains at its carboxy terminus a stretch of 27 residues, which are not observed in any h6LIMo isoforms. This is due to the usage of exon 7 in a different reading frame.

3.5. Differences between the expression of h6 and m17 LIMo genes

In order to confirm that the promoter sequences published in the databases were correct, we performed two distinct PCRs with one reverse primer within the first exon of the human and mouse genes and a couple of forward primers located at different positions within the promoter regions. These PCR showed that the two fragments obtained for each gene had the expected size (data not shown). The analyses of the promoter regions of both genes clearly showed that the human and mouse promoters are only 47% identical over 986 sites analyzed (excluding gaps).

The comparison of exon 7 from mouse and human genes showed that in the mouse a sequence of 37 bp is missing (Fig. 7). In the human gene, this sequence contains two perfect repeats of

14 nucleotides (arrowheads, Fig. 7); furthermore, two palindromic sequences involving 12 nucleotides separated by seven nucleotides are found (sequences colored in red in Fig. 7).

3.6. Expression of m17TLP in TNCs and cortical cell lines

To determine whether m17TLP is expressed in TNCs and cortical cell lines, we used three methods: (1) PCR, (2) in situ hybridization, and (3) immunofluorescence confocal microscopy. m17TLP is not expressed in any of the cortical cell lines tested (data not shown). In situ hybridization was performed on thymus cryosections using digoxigenin-UTP-labeled riboprobes. While we detected the enzyme terminal deoxynucleotidyl transferase in thymocytes, we were unable to visualize m17TLP in cortical epithelial cells by this method.

In order to identify the m17TLP protein in various cells, we used the rabbit polyclonal antibodies produced by Kirchner and colleagues. These antibodies were raised against a GST-TLP fusion protein containing residues 78–115, a region found in the linker portion of the mouse protein, which is divergent from the three known CRPs. In order to assess the specificity of these affinity-purified antibodies, we tested them by immunoblot analysis of various mouse tissues. One specific band of 23 kDa was identified in the thymic stromal cell lysate as found by Kirchner et al. [5], and not in kidney, ovary and heart. Furthermore, these purified antibodies do not give any significant staining of isolated thymocytes as measured by flow cytometry (data not shown). Using these affinity-purified rabbit anti-m17TLP antibodies, we found on thymus cryosections that m17TLP is expressed in cortical epithelial cells mostly near the corticomedullary junction and not in the medulla as previously described by Kirchner (data not shown). As shown in Fig. 8, on isolated thymic stromal cells, TNC are labeled with anti-m17TLP antibodies. The gallery (Fig. 8 panel C) reveals cavities, which contain unlabeled cells: those cells are known to be thymocytes. However, in our preparations, not all TNCs and stroma cells were labeled with the affinity-purified anti-m17TLP antibodies. In all experiments, staining controls were included, i.e. rabbit pre-immune serum as well as fluoresceinated secondary antibodies.

These antibodies were also used to compare human and mouse cell lysates by immunoblot analysis. While a specific band of 23 kDa was identified in the mouse thymic stromal cell lysate, no specific bands were detected in the human lysates from skeletal muscle, ovary testis and heart. An immunoblot control was performed on human and mouse cell lysates using an anti-human MAP-kinase; a specific band corresponding to the MAP-kinase was found in all human and mouse tissues tested (data not shown). Thus, the affinity-purified rabbit anti-m17TLP antibodies react with the m17TLP protein only.

4. Discussion

We have identified by RDA a LIMo, which is expressed in a subpopulation of TECs and TNCs in the mouse species, while in humans, the orthologous molecule is expressed in most tissues except skeletal muscle. We have identified three splice variants in the mouse, while four were detected in the human. Two of the mRNA isoforms of the m17TLP were previously identified [5]. Here, we describe a new variant, which is also expressed in the thymus. This variant uses exon 8 in a reading frame different from the mouse isoform A producing a carboxy-terminal domain of 27 residues bearing no sequence homology with the alternate carboxy-terminal sequences (Fig. 6). So far, three distinct CRPs have been identified: CRP1 is expressed in visceral smooth-muscle cells [23], CRP2 in vascular smooth-muscle, whereas CRP3 is found in striated muscle only [24,25]. It is postulated that their main function is to contribute to cytoskeleton dynamics. Sequence comparisons show that CRPs are close relatives of m17 and h6LIMo. It seems that CRP2 is the closest one (62% identity at the protein level). Besides, the second LIM domain of CRP2 is encoded by two exons of 95 and 58 bp, and the LIM domains

of the proteins described here are also encoded by exons with the same length, phase and symmetry.

Three-dimensional solution structures of CRP1 [26] and CRP2 [27] have shown that the two LIM domains are independent modules which do not interact directly and are coupled by a flexible linker in both molecules. The CRPs have the capacity to interact with specific proteins, as these CRPs have two LIM domains, it is postulated that they act as adapters bridging two distinct proteins. Zyxin and α-actinin were identified as binding partners of the three CRPs [1,8,28]. Harper et al. [29] have mapped the α-actinin binding site of CRP1 to a glycine-rich sequence located outside the N-terminal LIM domain. By site-directed mutagenesis on this 18-residue-long sequence, they showed that a lysine (K65) is essential for the interaction of α-actinin with CRP1. The m17TLP is not associated with actin in TECs [5]. This strongly suggests that m17TLP does not bind to α-actinin which cross-links actin. The absence of interaction of m17TLP with α-actinin is consistent with the observation that the N-terminal glycine repeat of m17TLP contains a leucine instead of lysine (K65) in the homologous sequence of CRP1. In order to determine whether zyxin is a binding partner of the m17TLP, we first tested its expression in thymus stroma and in 3T3 fibroblasts (as positive control) by PCR. While zyxin was found in 3T3 cells, it was absent from thymus stroma (data not shown). Thus, the m17TLP biological function may be distinct from the other known CRPs even though they share extensive homologies.

It is also striking that the h6LIMo is found in most tissues except skeletal muscle. A clear explanation for the divergent pattern of expression of m17TLP and h6LIMo is not available. However, the comparison of promoter regions of both genes showed 47% homology only over 980 sites analyzed. This suggests that the expression of both genes has diverged in these species. A more detailed analysis of the mouse gene promoter is needed to explain its restricted expression in a subset of cortical epithelial cells near the thymic corticomedullary junction.

When we analyzed the sequences of the h6LIMo and m17TLP genes, we found a difference in exon 7. In the mouse exon, a 37-bp sequence is lacking when compared to the corresponding human exon. This sequence generates the polypeptide sequence DGMYMPEHVWHV found in the human isoforms B and C only (Fig. 7, underlined sequence). The absence of this palindromic sequence in the mouse exon 7 may be due to the formation of a secondary structure leading to its removal from the mouse gene. Such a process has been observed in other instances such as in deletion mutations at the hypoxanthine-guanine phosphoribosyl transferase locus in human T lymphocytes [30] or in deletions in the APRT gene of Chinese hamster ovary cells [31]. Glickman and Ripley [32] have proposed a model to explain deletion mutations in which palindromic and quasipalindromic DNA sequences enable the formation of secondary structures that are removed by deletion. In the human and mouse CRP sequences, the polypeptide LSPS(S/N)FSPPRPRTGL found in the linker portion of the human and mouse proteins is divergent from the three known CRPs. This sequence does not correspond to any known protein motifs, and its potential function remains to be established. Interestingly, the rabbit polyclonal anti-m17TLP antiserum, raised by Kirchner and colleagues against a fusion protein containing residues 78–115 from the m17TLP linker, does not react with the h6LIMo. As can be seen in Fig. 6, two clusters of residues located on either side of the LSPS(S/N) FSPPRPRTGL sequence are different in m17TLP and h6LIMo proteins.

The expression of the m17TLP in a subpopulation of TECs and TNCs is clearly established when using anti-TLP affinity-purified antibodies. The expression of m17TLP is confirmed to a subset of TNC. As TNC have been found in two different areas of the thymus (reviewed in [33]), the outer cortex and the cortico-medullary junction, one may hypothesize that only the subset found at the cortico-medullary junction expresses m17TLP. Another explanation is that m17TLP is restricted to a particular developmental stage of TNC.

In summary, the results of these studies show that while m17TLP and h6LIMo genes present extensive homologies their tissue distribution is strikingly different. This is probably related to the weak homology of their promoter sequences. The highly restricted expression of m17TLP to a subpopulation of TEC and TNC makes one wonder whether m17TLP and h6LIMo have a similar function. The absence of zyxin in the thymic stroma and the inability of m17TLP to interact with actin [5] suggest that this CRP could bind to protein partners other than those identified for CRP1, 2 and 3. However, one could hypothesize that m17TLP shares some functions with the CRPs: involvement in adhesion plaques (CRP1) and organization of the actin cytoskeleton (the three CRPs). Thus, m17TLP could contribute to the binding of TECs to the thymic matrix, although through different molecular partners than those used by CRPs. Thus, the decrease in thymocyte numbers which is observed in m17TLP$^{-/-}$ could be due to the disappearance of m17TLP-positive TEC. The importance of TNC complex in the maintenance of thymocyte cellularity is strengthened by the observation that in *T. cruzi* infection, a trypomastigote-derived transialidase is involved in the thymic involution found during the acute phase of Chagas'disease [18]. This transialidase was shown to mediate apoptosis in the nurse cell complex [18].

Acknowledgments

Jean Kanellopoulos is supported by a grant from La Fondation pour la Recherche Médicale.

Abbreviations

CRP	cystein-rich protein
CTES	clusters of thymic epithelial staining
h6LIMo	human chromosme 6 LIM-only protein
LIMo	LIM-only protein
MHC	major histocompatibility complex
m17TLP	mouse chromosome 17 thymus LIM-only protein
TEC	thymic epithelial cells
TNC	thymic nurse cells
RDA	representational difference analysis

References

1. Sadler I, Crawford AW, Michelsen JW, Beckerle MC. Zyxin and cCRP: two interactive LIM domain proteins associated with the cytoskeleton. J Cell Biol 1992;119:1573–1587. [PubMed: 1469049]
2. Sanchez-Garcia I, Rabbitts TH. The LIM domain: a new structural motif found in zinc-finger-like proteins. Trends Genet 1994;10:315–320. [PubMed: 7974745]
3. Gill GN. The enigma of LIM domains. Structure 1995;3:1285–1289. [PubMed: 8747454]
4. Bach I. The LIM domain: regulation by association. Mech Dev 2000;91:5–17. [PubMed: 10704826]
5. Kirchner J, Forbush KA, Bevan MJ. Identification and characterization of thymus LIM protein: targeted disruption reduces thymus cellularity. Mol Cell Biol 2001;21:8592–8604. [PubMed: 11713292]
6. Schmeichel KL, Beckerle MC. The LIM domain is a modular protein-binding interface. Cell 1994;79:211–219. [PubMed: 7954790]
7. Pomies P, Macalma T, Beckerle MC. Purification and characterization of an alpha-actinin-binding PDZ-LIM protein that is up-regulated during muscle differentiation. J Biol Chem 1999;274:29242–29250. [PubMed: 10506181]

8. Beckerle MC. Zyxin: zinc fingers at sites of cell adhesion. Bioessays 1997;19:949–957. [PubMed: 9394617]
9. Boyd RL, Tucek CL, Godfrey DI, Izon DJ, Wilson TJ, Davidson NJ, Bean AG, Ladyman HM, Ritter MA, Hugo P. The thymic microenvironment. Immunol Today 1993;14:445–459. [PubMed: 8216723]
10. Wekerle H, Ketelsen UP, Ernst M. Thymic nurse cells. Lymphoepithelial cell complexes in murine thymuses: morphological and serological characterization. J Exp Med 1980;151:925–944. [PubMed: 6966312]
11. Penninger J, Hala K, Wick G. Intrathymic nurse cell lymphocytes can induce a specific graft-versus-host reaction. J Exp Med 1990;172:521–529. [PubMed: 2142720]
12. Lorenz RG, Allen PM. Thymic cortical epithelial cells can present self-antigens in vivo. Nature 1989;337:560–562. [PubMed: 2915706]
13. Ritter MA, Sauvage CA, Cotmore SF. The human thymus microenvironment: in vivo identification of thymic nurse cells and other antigenically-distinct subpopulations of epithelial cells. Immunology 1981;44:439–446. [PubMed: 7033113]
14. Andrews P, Boyd RL. The murine thymic nurse cell: an isolated thymic microenvironment. Eur J Immunol 1985;15:36–42. [PubMed: 2578399]
15. Defresne MP, Plum J, De Smedt M, Boniver J. Enzyme analysis of thymic nurse cells. Thymus 1988;11:221–230. [PubMed: 3140433]
16. Aguilar LK, Aguilar-Cordova E, Cartwright J Jr, Belmont JW. Thymic nurse cells are sites of thymocyte apoptosis. J Immunol 1994;152:2645–2651. [PubMed: 8144872]
17. Hiramine C, Nakagawa T, Hojo K. Murine nursing thymic epithelial cell lines capable of inducing thymocyte apoptosis express the self-superantigen Mls-1a. Cell Immunol 1995;160:157–162. [PubMed: 7842482]
18. Mucci J, Hidalgo A, Mocetti E, Argibay PF, Leguizamon MS, Campetella O. Thymocyte depletion in *Trypanosoma cruzy* infection is mediated by trans-sialidase-induced apoptosis on nurse cell complex. Proc Natl Acad Sci USA 2002;99:3896–3901. [PubMed: 11891302]
19. Lisitsyn N, Wigler M. Cloning the differences between two complex genomes. Science 1993;259:946–951. [PubMed: 8438152]
20. Hubank M, Schatz DG. Identifying differences in mRNA expression by representational difference analysis of cDNA. Nucleic Acids Res 1994;22:5640–5648. [PubMed: 7838717]
21. Oliveira-dos-Santos AJ, Penninger JM, Rieker-Geley T, Matsumoto G, Mak TM, Wick G. Thymic heterotypic cellular complexes in gene-targeted mice with defined blocks in T cell development and adhesion molecule expression. Eur J Immunol 1998;28:2882–2892. [PubMed: 9754575]
22. Frazer JK, Pascual V, Capra JD. RDA of lymphocyte subsets. J Immunol Methods 1997;207:1–12. [PubMed: 9328581]
23. Henderson JR, Macalma T, Brown D, Richardson JA, Olson EN, Beckerle MC. The LIM protein, CRP1, is a smooth muscle marker. Dev Dyn 1999;214:229–238. [PubMed: 10090149]
24. Arber S, Halder G, Caroni P. Muscle LIM protein, a novel essential regulator of myogenesis, promotes myogenic differentiation. Cell 1994;79:221–231. [PubMed: 7954791]
25. Jain MK, Kashiki S, Hsieh CM, Layne MD, Yet SF, Sibinga NE, Chin MT, Feinberg MW, Woo I, Maas RL, Haber E, Lee ME. Embryonic expression suggests an important role for CRP2/SmLIM in the developing cardiovascular system. Circ Res 1998;83:980–985. [PubMed: 9815145]
26. Yao X, Perez-Alvarado GC, Louis HA, Pomies P, Hatt C, Summers MF, Beckerle MC. Solution structure of the chicken cysteine-rich protein, CRP1, a double-LIM protein implicated in muscle differentiation. Biochemistry 1999;38:5701–5713. [PubMed: 10231520]
27. Konrat R, Krautler B, Weiskirchen R, Bister K. Structure of cysteine- and glycine-rich protein CRP2. Backbone dynamics reveal motional freedom and independent spatial orientation of the lim domains. J Biol Chem 1998;273:23233–23240. [PubMed: 9722554]
28. Louis HA, Pino JD, Schmeichel KL, Pomies P, Beckerle MC. Comparison of three members of the cysteine-rich protein family reveals functional conservation and divergent patterns of gene expression. J Biol Chem 1997;272:27484–27491. [PubMed: 9341203]
29. Harper BD, Beckerle MC, Pomies P. Fine mapping of the alpha-actinin binding site within cysteine-rich protein. Biochem J 2000;350:269–274. [PubMed: 10926853]

30. Osterholm AM, Bastlova T, Meijer A, Podlutsky A, Zanesi N, Hou SM. Sequence analysis of deletion mutations at the HPRT locus of human T-lymphocytes: association of a palindromic structure with a breakpoint cluster in exon 2. Mutagenesis 1996;11:511–517. [PubMed: 8921514]

31. Nalbantoglu J, Hartley D, Phear G, Tear G, Meuth M. Spontaneous deletion formation at the aprt locus of hamster cells: the presence of short sequence homologies and dyad symmetries at deletion termini. EMBO J 1986;5:1199–1204. [PubMed: 3015589]

32. Glickman BW, Ripley LS. Structural intermediates of deletion mutagenesis: a role for palindromic DNA. Proc Natl Acad Sci USA 1984;81:512–516. [PubMed: 6582506]

33. Pezzano M, Samms M, Martinez M, Guyden J. Questionable thymic nurse cell. Microbiol Mol Biol Rev 2001;65:390–403. [PubMed: 11528002]

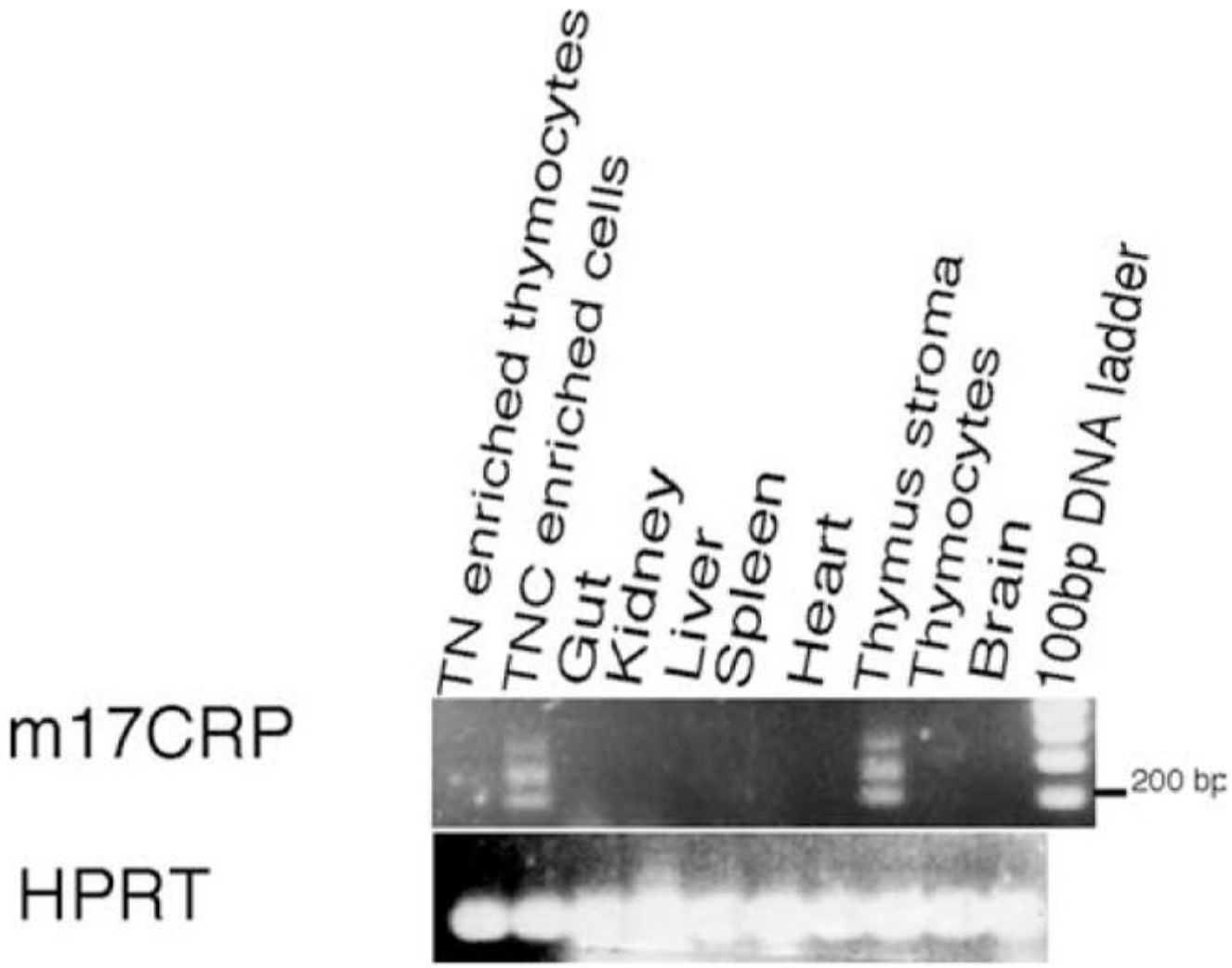

Fig. 1.

In the upper panel, PCR products are analyzed on 2% agarose gel. Three isoforms of m17TLP are identified in thymus stroma and thymic epithelial enriched cells. TN enriched thymocytes stand for triple-negative ($CD4^-$ $CD8^-$ $CD25^-$) enriched thymocytes. The lower panel shows HPRT PCR products as controls.

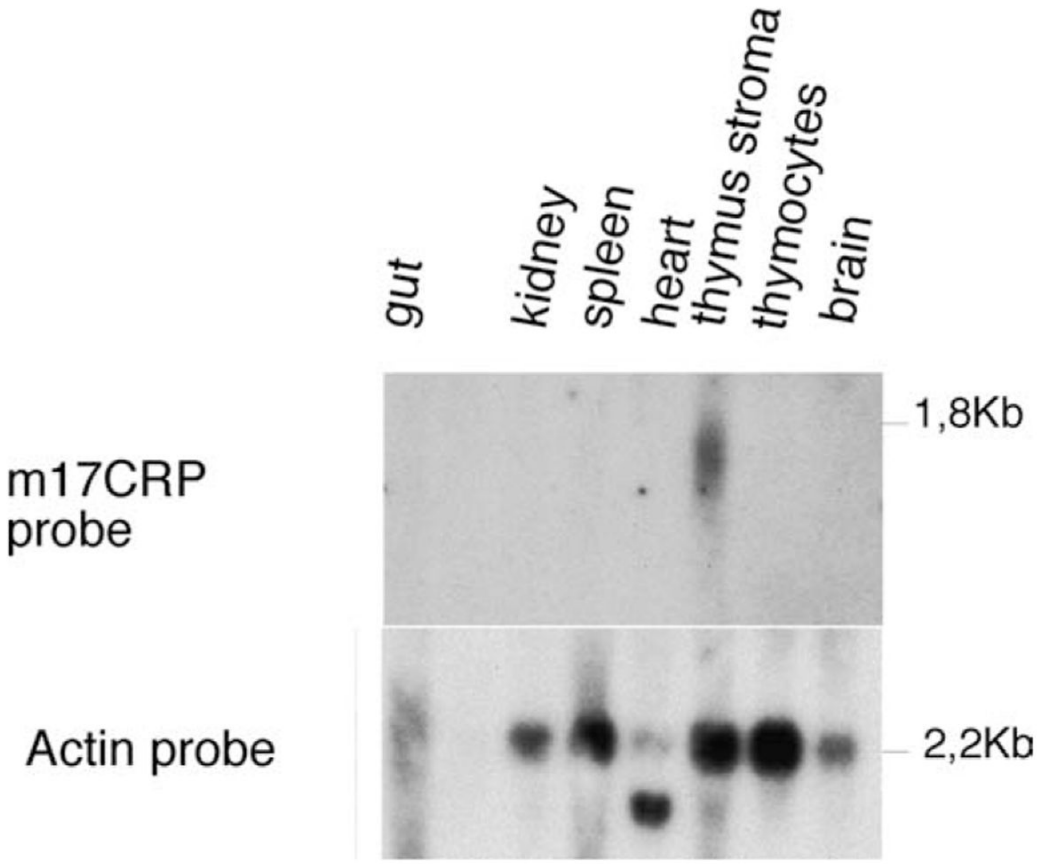

Fig. 2.
Northern analysis of m17TLP mRNA in different tissues. One specific band is detected in thymus stroma only, while actin messengers are observed in all tissues tested.

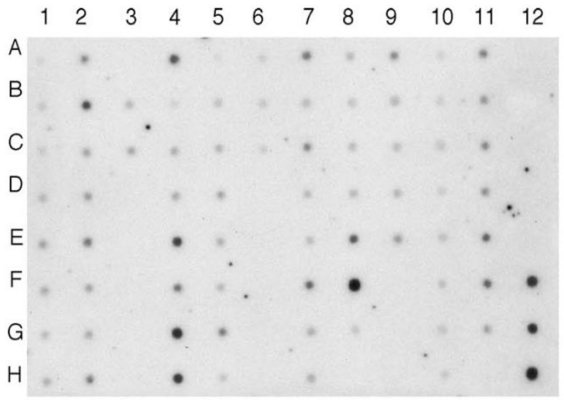

panel A

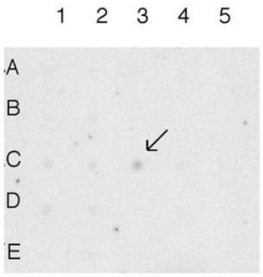

panel B

	1	2	3	4	5	6	7	8	9	10	11	12
A	whole brain	cerebellum, left		heart	esophagus	colon, transverse	kidney	lung	liver	leukemia, HL-60	fetal brain	yeast total RNA
B	cerebral cortex	cerebellum, right	accumbens nucleus	aorta	stomach	colon, desending	skeletal muscle	placenta	pancreas	HeLa S3	fetal heart	yeast rRNA
C	frontal lobe	corpus callosum	thalamus	atrium, left	duodenum	rectum	spleen	bladder	adrenal gland	leukemia, K-562	fetal kidney	*E. coli* rRNA
D	parietal lobe	amygdala		atrium, right	jejunum		thymus	uterus	thyroid gland	leukemia, MOLT-4	fetal liver	*E. coli* DNA
E	occipital lobe	caudate nucleus		ventricle, left	ileum		peripheral blood leukocyte	prostate	salivary gland	Burkitt's lymphoma, Raji	fetal spleen	Poly r(A)
F	temporal lobe	hippo-campus		ventricle, right	ilocecum		lymph node	testis		Burkitt's lymphoma, Daudi	fetal thymus	human C_0t -1 DNA
G	p. g.* of cerebral cortex	medulla oblongata		inter-ventricular septum	appendix		bone morrow	ovary		colorectal adeno-carcinoma, SW480	fetal lung	human DNA 100 ng
H	pons	putamen		apex of the heart	colon, ascending		trachea			lung carcinoma, A549		human DNA 500 ng

* acentral gyrus

	1	2	3	4	5	6
A	brain	eye	liver	lung	kidney	
B	heart	skeletal muscle	smooth muscle			
C	pancreas	thyroid	thymus	submax. gland	spleen	
D	testis	ovary	prostate	epididy-mus	uterus	
E	embryo 7 days	embryo 11 days	embryo 15 days	embryo 17 days		

Fig. 3.

Dot blot analysis of h6 and m17 LIMo expression in different tissues. As observed in panel A, human LIMo is strongly detected in testis and heart, more weakly in fetal thymus and spleen, prostate and lymph node. Panel B, mouse 17 TLP is very weakly detected in thymus only.

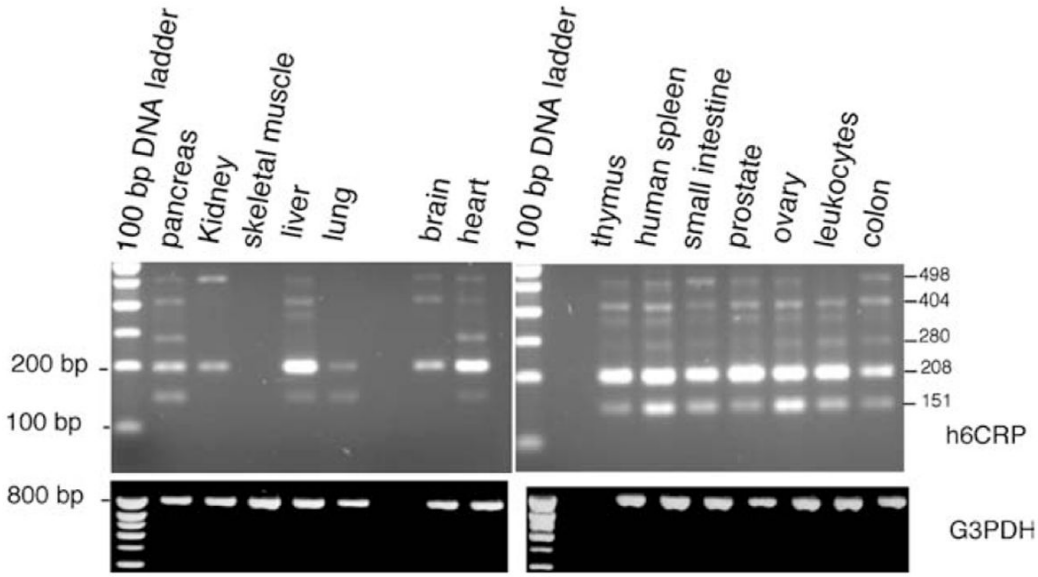

Fig. 4.

Comparison of tissue expression patterns of h6LIMo and G3PDH in multiple tissue cDNA. Each cDNA corresponding to a given tissue was used as a PCR template with the human specific primers or with the control G3PDH primers. Upper panels, the human LIMo products are analyzed. Five bands of 151, 208, 280, 404 and 498 bp are found in pancreas. Various LIMo isoforms are detected in all tested tissues except in skeletal muscle. The 208-bp isoform is the most abundant one. Lower panels show the G3PDH control PCR products.

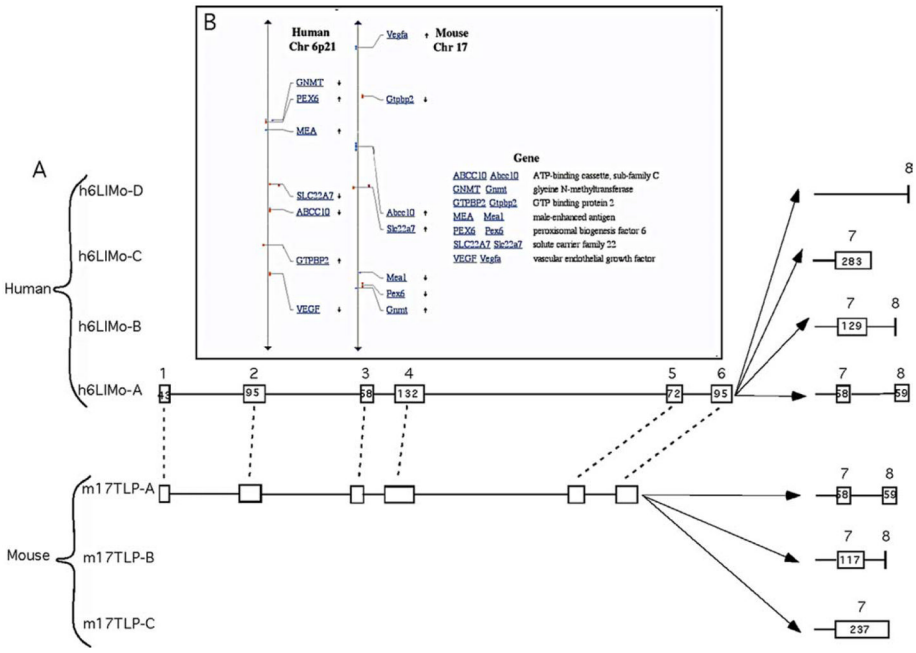

Fig. 5.

Comparison of the h6LIMo and m17TLP genes. **PanelA**. The h6 and m17 LIMo genes contain eight exons and seven introns. The distinct splice variants are produced by alternative splicing of exon 7 in mouse and human except for the human isoform D. In the latter, exon 7 is not used and exon 8 contributes for one amino acid only. Human isoform A comprises exon 7 from bp 2669 to 2726 (numbering of nucleotide starts at A of ATG) and a portion of exon 8 (2918–2954). B isoform uses exon 7 from bp 2669 to 2797, and exon 8 contributes to only one amino acid. The splice variant C involves the complete exon 7 only.

Panel B. Alignment between the mouse and human chromosome segments containing the h6LIMo and m17TLP genes. ABCC10, Abcc10 ATP-binding cassette, subfamily C; GNMT, Gnmt glycine N-methyltransferase; GTPBP2, Gtpbp2 GTP binding protein 2; MEA, meal male-enhanced antigen; PEX6, Pex6 peroxisomal biogenesis factor 6; SLC22A7, Slc22a7 solute carrier family 22; VEGF, Vegfa vascular endothelial growth factor.

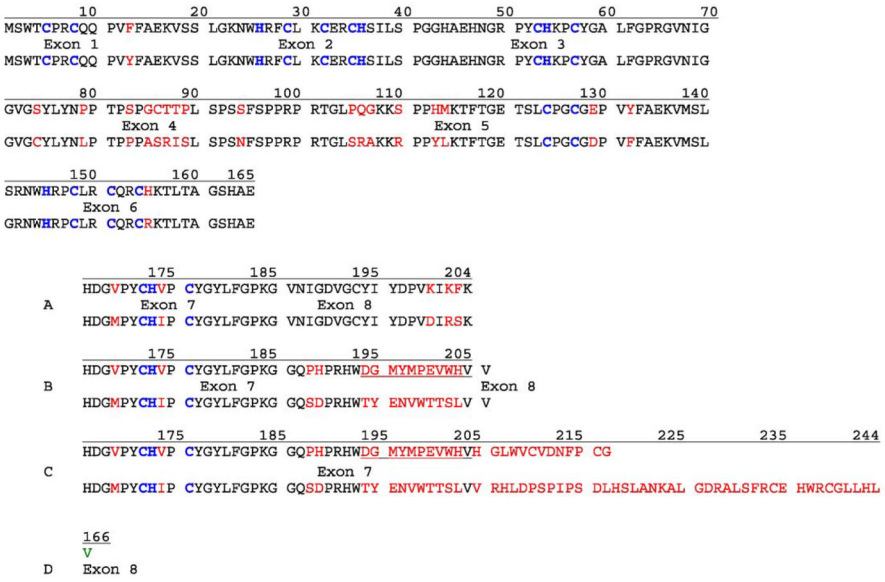

Fig. 6.

Alignment of amino acid sequences of h6LIMo and m17TLP splice variants; the amino acid residues (red) which differ in human (upper sequence) and mouse (lower sequence) sequences. Outline of the cystein and histidine residues (purple) which are zinc coordinated in the LIM fingers. Under each sequence, the exon numbers are indicated. The first 175 amino acid residues are common to all splice variants. The distinct isoforms A, B, C and D are indicated on the left side of the sequences. The amino acid residues encoded by the double repeats in the human sequence are underlined in red. GenBank accession numbers AY555741, AY555742, AY555743, AY555744 and AY555745 correspond to the h6LIMo isoformA, B, C, D and to the m17TLP isoform C cDNAs, respectively.

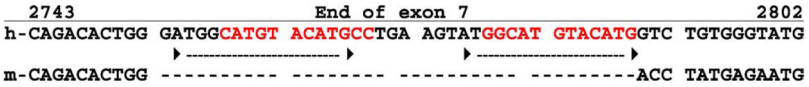

Fig. 7.

Comparison of the nucleotide sequences from h6LIMo and m17TLP exon 7. A stretch of the nucleotide sequence of the human exon 7 (h), from nucleotide 2743 to 2802, is aligned with the corresponding sequence of the mouse exon 7 (m). A stretch of 37 nucleotides is absent in the mouse gene. In the human sequence, two perfect repeats are outlined (dashed arrows), and the 12 nucleotides of the palindromic sequences are colored in red.

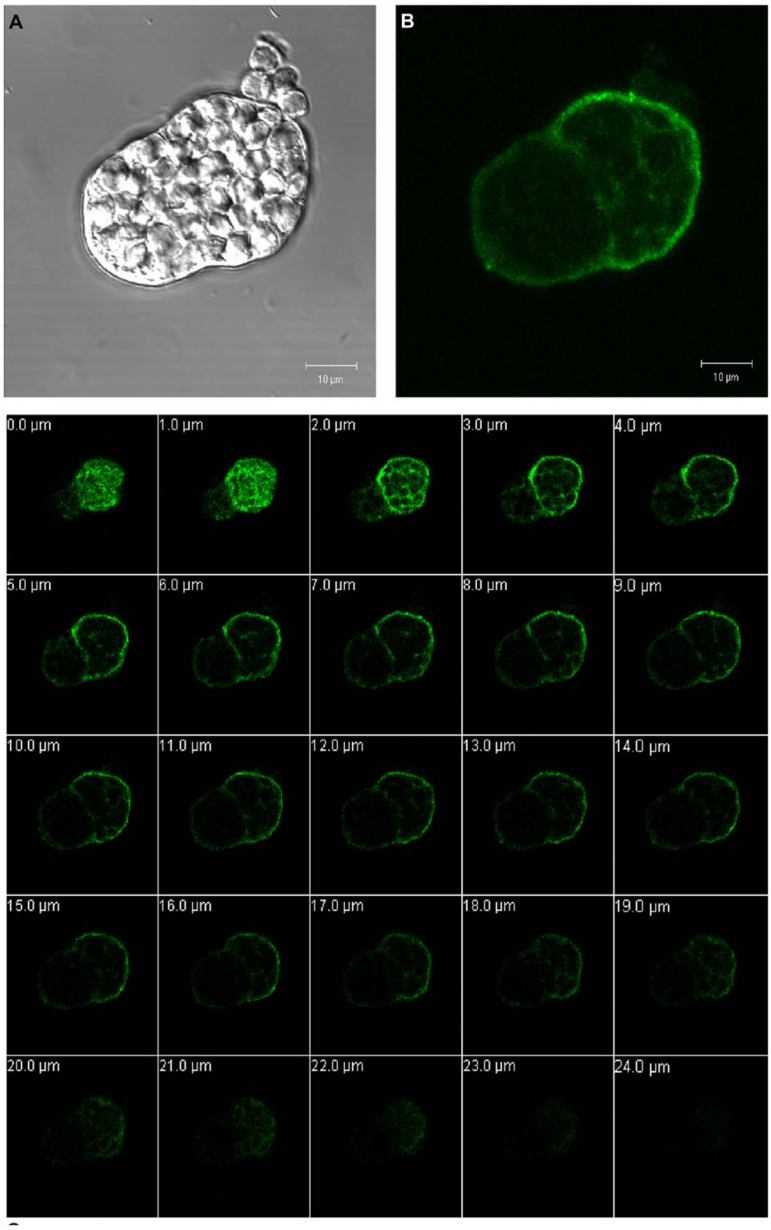

Fig. 8.

TNCs from C57BL/6 mice were stained with affinity-purified anti-TLP antibodies (as described in Section 2). In (A), the TNC is shown in interferential Nomarsky. In (B), m17TLP distribution was visualized by confocal microscopy. In (C) 20 sections acquired by confocal scanning microscopy are presented. The TNC size is 47 µm in length, 22 µm in width and the "vacuoles" containing thymocytes are about 6.3 µm in diameter.